Stanislav Bartoň

Aerodynamic deceleration at velocities near the escape velocity

In: Jan Chleboun and Jan Papež and Karel Segeth and Jakub Šístek and Tomáš Vejchodský (eds.): Programs and Algorithms of Numerical Mathematics, Proceedings of Seminar. Hejnice, June 23-28, 2024. Institute of Mathematics, Czech Academy of Sciences, Prague, 2025. pp. 7–15.

Persistent URL: http://dml.cz/dmlcz/703223

Programs and Algorithms of Numerical Mathematics 22
J. Chleboun, J. Papež, K. Segeth, J. Šístek, T. Vejchodský (Eds.)
Institute of Mathematics CAS, Prague 2025

AERODYNAMIC DECELERATION AT VELOCITIES NEAR THE ESCAPE VELOCITY

Stanislav Bartoň

Opole University of Technology
Prószkowska Street 76, 45-758 Opole, Poland
s.barton@po.edu.pl

Abstract: This article presents basic procedures for calculating the trajectory of a spaceship that uses only the Earth's atmosphere to reduce its speed, allowing it to land on the Earth's surface successfully. The first flight of the `ARTEMIS` program, which took place from November 16 to December 11 2022, was used as a template for the calculations. All calculations are performed in the symbolic algebra program Maple. To simplify the calculations, forces that have a less significant impact on the shape of the trajectory, such as the gravitational influence of the Sun and Moon, the rotation of the Earth, and its non-spherical shape, were neglected. To conserve space, only the essential components of the solution are shown, given the intensive calculations involved. The commands used to produce the graphics are not included.

Keywords: Newton's equations of motion, aerodynamic drag, atmospheric density, gravitational field, iteration method, Maple

MSC: 34A34, 68W30, 76-04

1. Introduction

The Artemis I mission inspired this article, which expands on the mathematical models the author developed in 2002, see [3].

Spacecraft landings are among the most demanding phases of space missions. Lunar missions necessitate precise trajectories, mandating frequent course corrections. Altering the spacecraft's direction and velocity during lunar orbit insertion and Earth return is also crucial. Fuel consumption is directly linked to the spacecraft's overall mass, meaning more fuel is required for final maneuvers if more is needed for mid-course corrections. Given the limited launch mass of rockets, fuel for course corrections is also limited. To conserve fuel during atmospheric reentry, spacecraft utilize aerodynamic drag, a process that doesn't consume fuel.

All input variables for the forthcoming calculations are expressed numerically using SI base or derived units. To conserve space, only numerical values will be

DOI: 10.21136/panm.2024.01

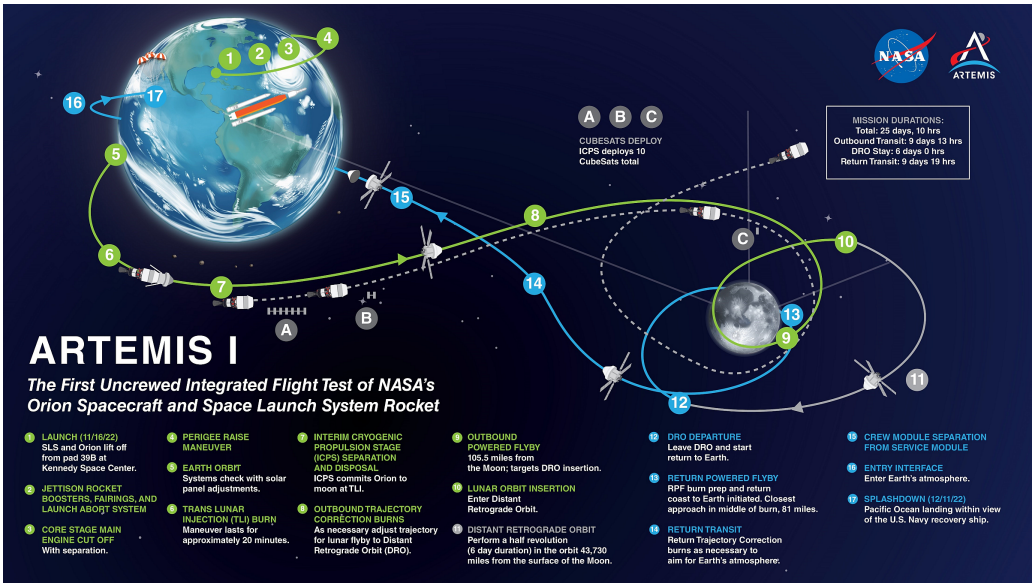

Figure 1: `ARTEMIS I` Mission Map, [1].

presented. For spacecraft returning from lunar trajectories, reentry speeds approach the escape cosmic velocity, $\approx 11.2\text{e}3$. Martian return speeds are significantly higher, around $\approx 21\text{e}3$. The Orion spacecraft during the ARTEMIS 1 mission reentered at $W = 10.7\text{e}3$, detailed in [2] and see Fig. 1.

2. Derivation of equations of motion

We start with the fundamental form of Newton's equations of motion:

$$\left[\frac{d^2\,x(t)}{dt^2}, \frac{d^2\,y(t)}{dt^2}\right] = \frac{1}{M}\,\left[F_x\left(x(t), y(t)\right), F_y\left(x(t), y(t)\right)\right], \tag{1}$$

where x and y represent rectangular coordinates with the origin at the Earth's center. The positive x-axis points towards the initial point of the landing trajectory, located at $[x_0, 0]\,, x_0 = 1\text{e}6$, where the spacecraft is at time $t = 0$ and $\vec{F}$ is the vector representing the total force acting on the spacecraft, which has a mass of $M = 1.00375\text{e}5$, see [5].

The primary forces acting on a descending spacecraft are the gravitational force $\vec{G} \equiv [G_x, G_y]$ and and aerodynamic drag $\vec{D} \equiv [D_x, D_y]$

$$|\vec{G}| = \frac{\kappa\,Me\,M}{r^2}, \qquad |\vec{D}| = \frac{C_x\,\rho(h)\,S\,V^2}{2}. \tag{2}$$

In these equations: $Me = 5.97\text{e}24$ is the mass of the Earth, $\kappa = 6.67\text{e}-11$, r is the distance of the spacecraft from the Earth's center, $C_x = 1.5$ is the spacecraft's drag coefficient, see [6], $S = 19.6$ is the spacecraft's frontal area, see [5] and V is the spacecraft's velocity.

The function describing the variation of atmospheric density ρ with altitude h above the Earth's surface is

$$\rho(h) = \mathrm{e}^{\left(\left(c_1\,h^2 - c_2\,h + c_3\right)\mathrm{He}(c_4 - h) - \frac{(c_5\,h - c_6)\mathrm{He}(h - c_4)}{h + c_7}\right)}, \text{ where } \begin{array}{ll} c_1 = 6.392146930\text{e}{-11} & c_5 = 3.502764072\text{e}1 \\ c_2 = 1.447577359\text{e}{-4} & c_6 = 1.41258792\text{e}6 \\ c_3 = 3.316213319\text{e}{-1} & c_7 = 5.494654461\text{e}4 \\ c_4 = 1.044139387\text{e}5 & \mathrm{He} = \text{Heaviside function} \end{array} . \quad (3)$$

The function $\rho(h)$, defined by equation (3), is a generalization of atmospheric density relationships found in [7]. The coefficients $c_1, \ldots, c_7$ were computed in Maple using a least squares fit to a nonlinear, piecewise defined regression model for atmospheric density, based on tabulated values in [4].

The following substitutions can now be used:

$$\begin{gathered} F_x = -G_x - D_x,\ F_y = -G_y - D_y,\ r = \sqrt{x(t)^2 + y(t)^2},\ h = r - RE, \\ V = \sqrt{\left(\frac{d\,x(t)}{dt}\right)^2 + \left(\frac{d\,y(t)}{dt}\right)^2},\ G_x = |G|\frac{x(t)}{r},\ G_y = |G|\frac{y(t)}{r},\ D_x = \frac{|D|}{V}\frac{d\,x(t)}{dt},\ D_y = \frac{|D|}{V}\frac{d\,y(t)}{dt} \end{gathered} , \quad (4)$$

where $RE = 6.378\text{e}6$ represents the Earth's radius. These substitutions, along with equations (2), (3) and the provided numerical values, can then be used in equation (1). Because of space limitations, we are unable to show the final form of these equations.

3. Calculation of the return trajectory in Maple

A description of the derivation of the equations of motion in Maple would be very lengthy and formally identical to the previous chapter. Therefore, we will assume that the equations of motion have already been derived in Maple from the substitutions (4), (3) and (2) into equation (1) and that this vector equation has been divided in Maple into two equations describing the motion in the x and y axes. These equations have been named `EQx` and `EQy` in Maple. Both equations form a system of ordinary nonlinear second-order differential equations. Their numerical solution and the search for the optimal return trajectory of the spacecraft are the subject of this part.

By the optimal return trajectory, we mean a trajectory that minimizes deceleration caused by aerodynamic drag. To quantify this deceleration, we introduce a new variable, `Ag` $= \frac{\sqrt{Dx^2 + Dy^2}}{g}$, representing the aerodynamic load factor in multiples of the standard gravitational acceleration, $g = 9.81$. A commonly used term for this quantity is g-force. Here, `Dx` and `Dy` represent the components of the aerodynamic drag force in the x and y directions, respectively.

If the g-force is maximal, then the condition for the existence of an extremum of a continuous function must hold: $\frac{d\,Ag(t)}{dt} = 0$ and the corresponding time t for which this condition is fulfilled can be found using the Newton-Raphson method. However, the complication lies in the very complex form of the variable `Ag`. It contains multiple occurrences of both $\frac{d\,x(t)}{dt}$ and $\frac{d\,y(t)}{dt}$ always within the arguments of nonlinear functions. Given that the use of the Newton-Raphson method requires

the computation of `Agt` $= \frac{d\,Ag(t)}{dt}$ and `Agtt` $= \frac{d^2\,Ag(t)}{dt^2}$ an analytical expression of these variables would be possible but practically unusable. The analytical expression of `Agtt` alone contains 66200 characters and occupies over 300 MB in Maple's memory.

However, we can still proceed with a numerical solution. To do this, we must first define the following initial conditions: `W:=1.07e4: Alpha:=78.0: RE:=6.378e6: x0:=RE+1e6: y0:=0`. These values represent the spacecraft's initial position at time $t = 0$ which is $[x0, y0]$, and its initial velocity `W`, which makes an angle of `Alpha` degrees with the direction towards the center of the Earth.

Once the initial conditions `Ini` are defined, we can numerically solve the system of equations `EQx` and `EQy` to obtain a solution `Ns`. This solution provides the values of the coordinates and their corresponding velocities at any given time, as demonstrated in the last line of the following code.

```
> alpha:=evalf(convert(Alpha*degrees,radians));
> Ini:=x(0)=x0,y(0)=0,D(x)(0)=-W*cos(alpha),D(y)(0)=W*sin(alpha):
> Ns:=dsolve({Ini,EQx,EQy},{x(t),y(t)},numeric):
> Ns(500.);
```

$$\left[t=500.0, x(t)=5249645.296, \frac{d\,x(t)}{dt}=-121.112, y(t)=3646265.675, \frac{d\,y(t)}{dt}=-73.279\right]$$

A slightly modified `Ns(tf)` procedure allows for the numerical computation of the third time derivatives of coordinates x and y at time `tf`. The resulting values are then substituted into variables `Agtt` and `Agt` with the aim of applying the Newton-Raphsson method to determine the maximum g-force and the corresponding time.

After deriving the equations of motion `EQx` and `EQy`, the general analytical expressions for the third time derivatives of the coordinates, `Xttt:=diff(rhs(EQx),t):` and `Yttt:=diff(rhs(EQx),t):`, must be obtained. Before initiating the iteration, the first element `SUNs:= Ns(tau)[2..-1]:` needs to be extracted from the output of `Ns`.

Now, the iterative procedure `AGmax` can be used to determine the exact time at which the maximum overload occurs. The input parameter for this procedure is an estimate of the time when we expect the maximum g-force to happen.

```
AGmax := proc(tau) global tau, SUNs;
   local dt, Xtts, Ytts, Xttts, Yttts, Agtts, Agts;
   dt:=1: SUNs:= Ns(tau)[2..-1]:
   while abs(dt)>1e-6 do:
      Xtts:=diff(x(t),t,t)=evalf(subs(SUNs,rhs(EQx)));
      Ytts:=diff(y(t),t,t)=evalf(subs(SUNs,rhs(EQy)));
      Xttts:=diff(x(t),t,t,t)=evalf(subs(Xtts,Ytts,SUNs,Xttt));
      Yttts:=diff(y(t),t,t,t)=evalf(subs(Xtts,Ytts,SUNs,Yttt));
      Agtts:=evalf(subs(Xttts,Yttts,Xtts,Ytts,SUNs,Agtt));
      Agts:=evalf(subs(Xtts,Ytts,SUNs,Agt));dt:=-Agts/Agtts;tau:=tau+dt;
   end do:
end proc:
```

Similarly, the landing time, i.e., the time at which the altitude $h = 0$, can be determined. The calculation is performed by the procedure `Tau`, again using the Newton-Raphson method. The input parameter of the procedure is the estimated landing time.

```
Tau := proc(T) local dt, tau;
   dt := 1.0; tau := T;
   while .1e-3 < abs(dt) do
      dt := subs(Ns(tau),-h/diff(h,t)); tau := tau+dt end do;
   tau
end proc;
```

Given the specified initial conditions, the trajectory can now be computed. The landing time, denoted by `t0 - #1`, is initially determined using the subroutine `Tau`. The trajectory is then visualized using the `odeplot` command and saved as `TR - #2`. Similarly, a plot of the overload versus time is generated and saved as `GT - #3`. The coordinates of the data points on this plot, represented as $[t, Ag]$, are extracted and stored in the matrix `MG - #4`. From this matrix, approximate values of the maximum g-forces and their corresponding times are determined and stored in `MMG - #5`. Considering the selected entry angle, multiple maxima, denoted by `nu - #6`, may exist.

A loop spanning lines `#7 - #11` processes the approximate value of each maximum. The subroutine `AGmax - #8` is employed to calculate the precise times corresponding to these maxima, and the exact g-force values are stored in `Agf - #9`. The ordered pairs [*time of maximum, maximum g-force*] are then collected into the list `AGF - #10`.

```
> t0:=Tau(t0);                                                    #1
> TR:=display(odeplot(Ns,[x(t)/RE,y(t)/RE],0..t0,numpoints=1000)): #2
> GT:=odeplot(Ns,[t,Ag],0..t0,numpoints=1000):                    #3
> MG:=convert(op(1,op(1,GT)),Matrix);                             #4
> MMG:=[seq(`if`(MG[i-1,2]<MG[i,2] and MG[i,2]>MG[i+1,2],
      [MG[i,1],MG[i,2]],NULL),i=2..999)];                         #5
> nu:=nops(MMG); AGF:=[];                                         #6
> for k from 1 by 1 to nu do                                      #7
>   tau:=MMG[k][1]; AGmax(tau);                                   #8
>   Agf:=evalf(subs(SUNs,Ag));                                    #9
>   AGF:=[AGF[],[tau,Agf]];                                       #10
> end do:                                                         #11
```

4. Calculation of the optimal trajectory

The optimal trajectory is designed to minimize the overload during aerodynamic braking while also considering the descent time. For this reason, it is advantageous to select an entry angle into the atmosphere that results in two overload peaks of equal magnitude. It is possible to find return trajectories with three or more g-force peaks, but following these trajectories results in circumnavigating the entire Earth

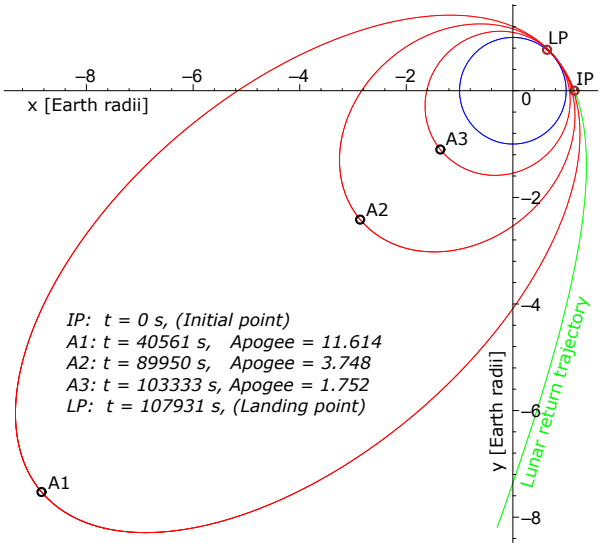

Figure 2: Trajectory with 3 g-force peaks.

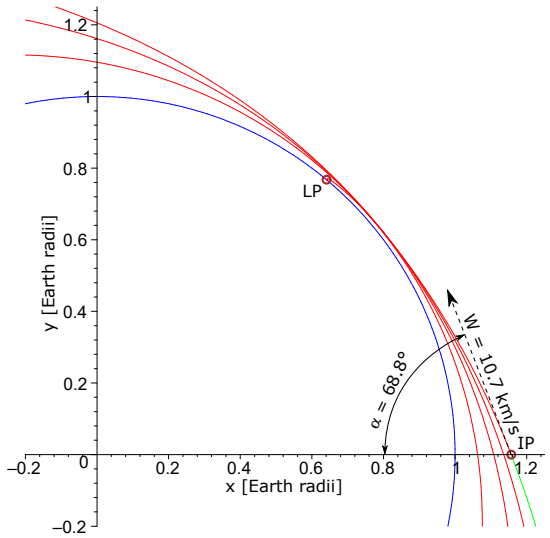

Figure 3: Detail.

on a high-apogee orbits, see Figures 2 and 3. This significantly increases the landing time. Therefore, these trajectories were rejected.

By following the procedure outlined in Section 3 and appropriately selecting the interval of the angle `Alpha` and the step size `dAlpha`, such an angle can be found very quickly, see Figure 4.

The optimal value is $\alpha = 68^\circ\,37'\,8.08'' \pm 0.04''$. Landing occurs at $t_0 = 847.93 \pm 0.01\,[s]$ from the moment the spacecraft was at the initial point. The maximum g-gorce is $Ag = 6.430 \pm 0.001\,[g]$ and the g-force peaks occur at times $t_1 = 443.33 \pm 0.01\,[s]$ and $t_2 = 550.94 \pm 0.01\,[s]$, see Figure 5. Figure 6 illustrates the dependence of a spacecraft's flight altitude on time, while Figure 7 depicts the time evolution of the spacecraft's velocity.

Figure 8 presents the dynamics of the final landing maneuver for the optimal angle as a 3D curve $[Ag(t), V(t), h(t)]$, along with its projections onto the $[Ag(t), V(t)]$, $[Ag(t), h(t)]$, and $[V(t), h(t)]$ planes.

5. Conclusion

The presented calculations underscore the critical role of precise navigation in spacecraft reentry. The range of angles α that guarantee a safe landing is exceptionally narrow. If the spacecraft deviates from the optimal value of $\alpha = 68^\circ\,37'\,8.08'' \pm 0.04''$ by $-3'\,50''$, the landing g-force will exceed 10g. A deviation of $-17'\,46''$ will result in a g-force exceeding 20g, which could have fatal consequences. Additionally, at low entry angles, the heat shield may not provide sufficient protection, as the rate of conversion of kinetic energy to thermal energy can be very high.

If the value of angle α increases by $10'\,21''$, the landing will occur after one day, or 86 400 seconds, after passing the initial point. If the deviation is $11'\,50''$, the

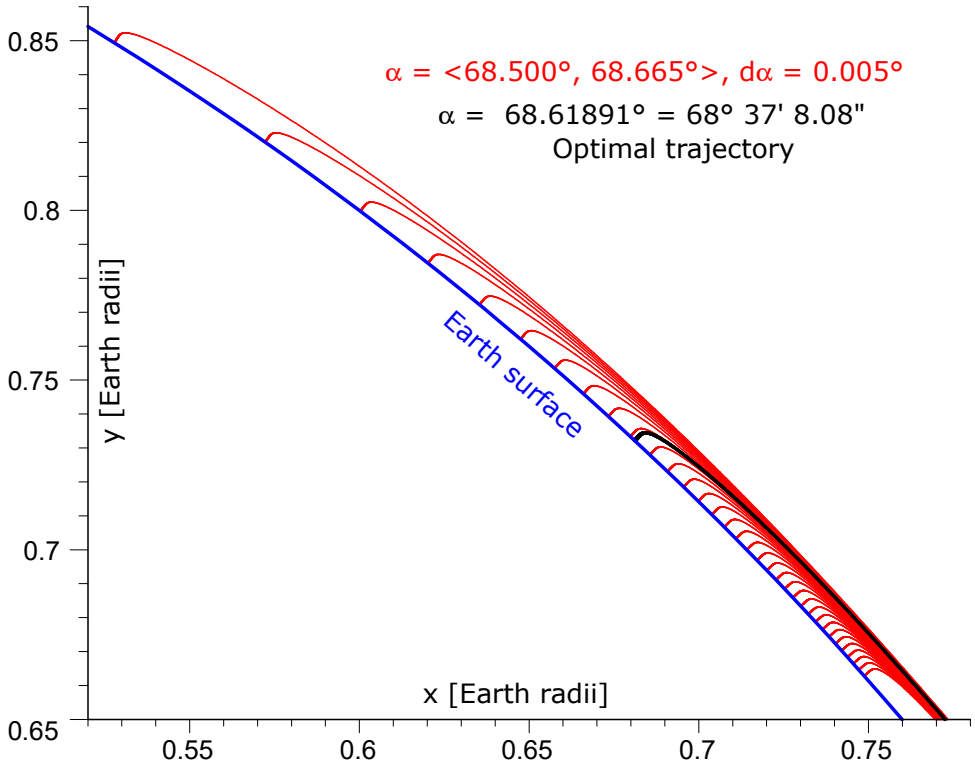

Figure 4: Landing trajectories.

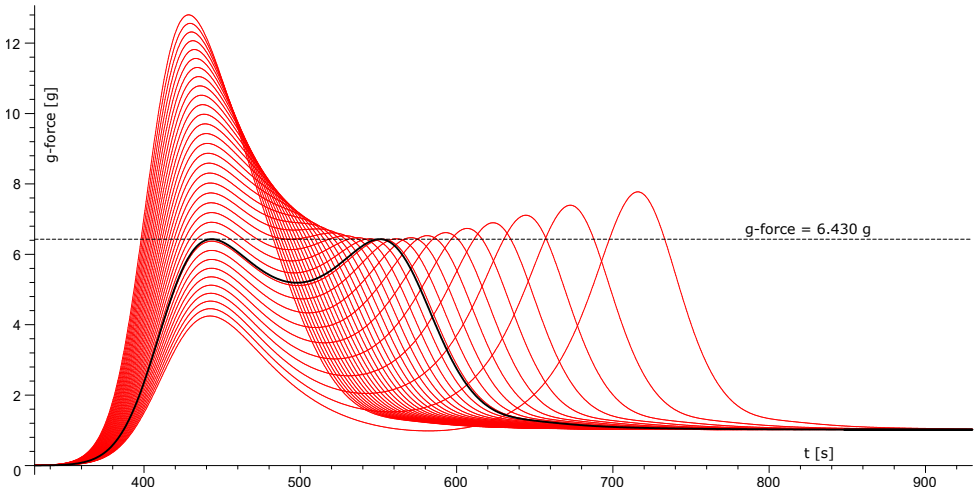

Figure 5: g-force as a function of the time.

landing will occur after two days. This means that a difference of one arcminute and twenty-nine arcseconds results in a full day extension of the flight time. This could be a significant complication for the spacecraft crew after separation from the service

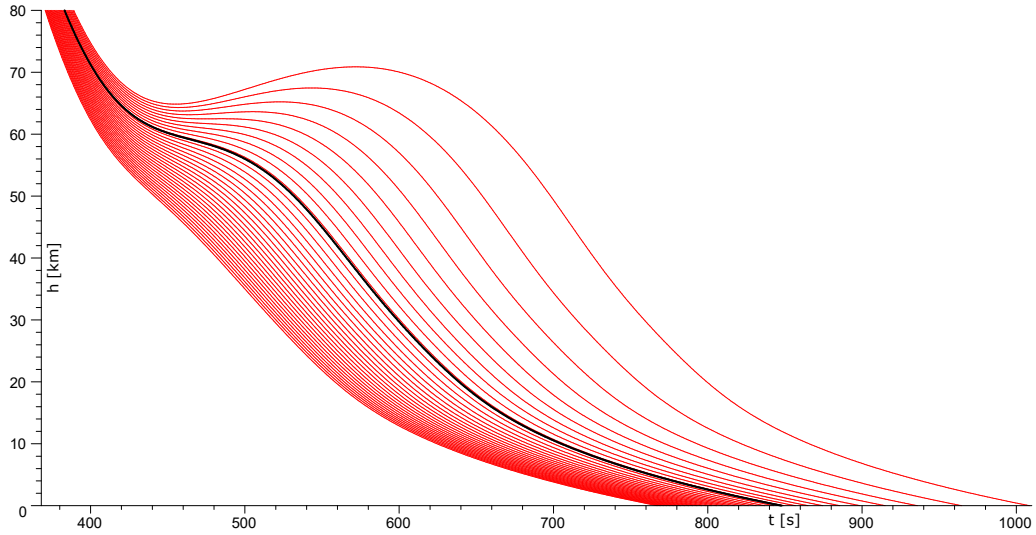

Figure 6: Flight height a function of the time.

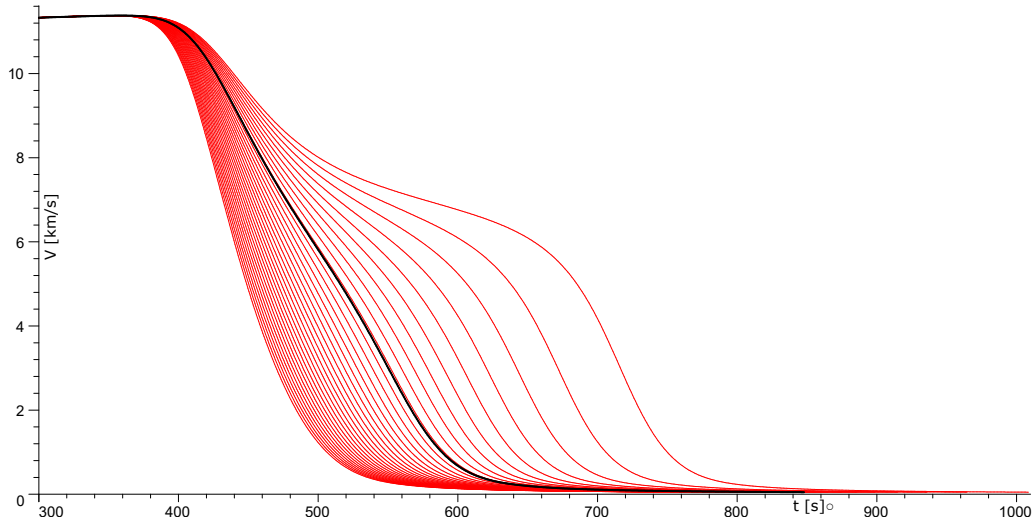

Figure 7: Flight velocity a function of the time.

module. Furthermore, increasing the deviation from the optimal angle leads to an exponential increase in landing time. If the spacecraft were to pass the initial point at a speed higher than the escape velocity, it would enter a solar orbit and never return to Earth. This is the case for spacecraft returning from interplanetary missions.

This means that the range of atmospheric entry angles is very narrow, approximately one quarter of a degree. Therefore, the accuracy and quality of mathematical modeling play a crucial role in solving this problem.

A Maple worksheet with all commands, including the generation of graphics, will be posted on the Maple application center in the near future.

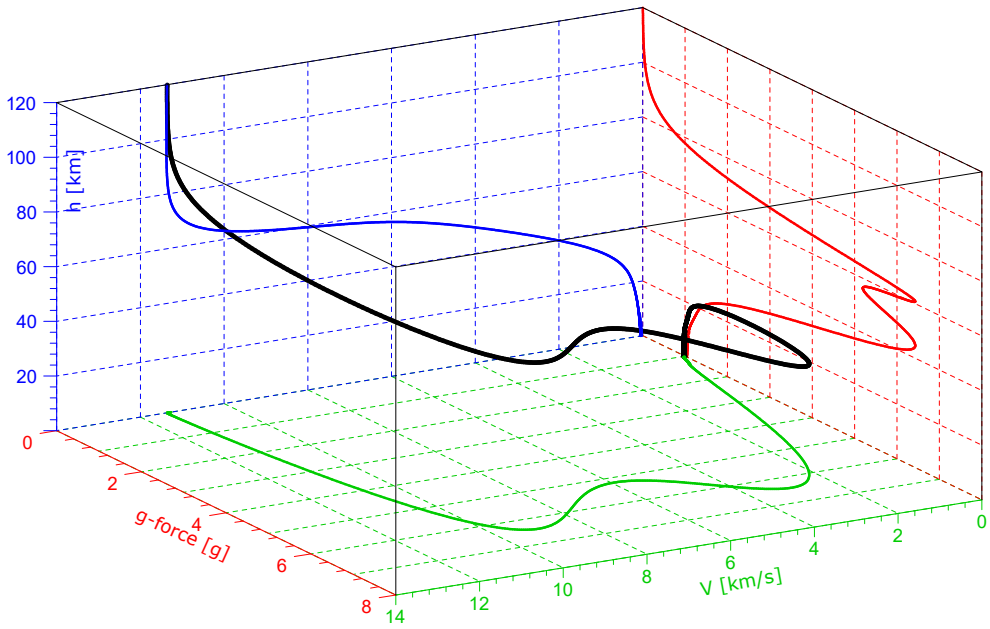

Figure 8: Landing dynamics.

References

[1] Artemis I.: Online, `https://en.wikipedia.org/wiki/Artemis_I`, last access 14/09/2024.

[2] Artemis I Mission map. Online, `https://www.nasa.gov/mission/artemis-i/`, last access 14/09/2024.

[3] Barton, S.: Modeling of atmospheric motion and astrodynamics. Online, `https://www.maplesoft.com/Applications/Detail.aspx?id=4309`, last access 14/09/2024.

[4] CRC handbook of chemistry and physics. D. R. Linde, (Ed.) Tables 14–13 and 14–14. CRC Press, 72nd edition, 1991.

[5] Owens, D. B. and Aubuchon, V. V.: Overview of Orion crew module and launch abort vehicle dynamic stability. American Institute of Aeronautics and Astronautics. Online, `https://ntrs.nasa.gov/api/citations/20110015371/downloads/20110015371.pdf`, last access 14/09/2024.

[6] Raj, C. A. S., Narasimhavaradhan, M., Vaishnavi, N., Arunvinthan, S., Alarjani, A. A., and Pillai S. N.: Aerodynamics of ducted re-entry vehicles. Chinese Journal of Aeronautics **33** (2020), 1837–1849, doi.org/10.1016/j.cja.2020.02.019.

[7] *U.S. standard atmosphere 1976.* Online, `https://ntrs.nasa.gov/api/citations/19770009539/downloads/19770009539.pdf`,
last access 14/09/2024.